

Crystallographic Analysis of Proeutectoid Ferrite/Austenite Interface and Interphase Precipitation of Vanadium Carbide in Medium-Carbon Steel

GORO MIYAMOTO, RYOTA HORI, BEHRANG POORGANJI,
and TADASHI FURUHARA

To clarify the mechanism of interphase precipitation of vanadium carbide (VC) in a medium-carbon steel, orientation relationships (ORs) and plane orientations of ferrite/austenite interfaces were investigated. It was found that a large part of grain boundary ferrite holds near-K-S OR with at least one side of austenite adjacent to grain boundary regardless of V addition. By the V addition, a fraction of grain boundary ferrite holding near the K-S OR with both sides of austenite is decreased remarkably. Furthermore, only non-K-S ferrite/austenite interfaces migrate dominantly in the V-added alloy in contrast to the V-free alloy. Ferrite/austenite interface orientations are not fixed crystallographically but are randomly distributed in terms of ferrite and austenite orientations. Those results do not agree with the ledge mechanism originally proposed by Honeycombe. Thus, it is proposed that the ledge mechanism is extended to the non-K-S interface, which partially consists of coherent and less-mobile interfaces.

DOI: 10.1007/s11661-013-1702-2

© The Minerals, Metals & Materials Society and ASM International 2013

I. INTRODUCTION

DURING proeutectoid ferrite (α) and pearlite transformation in steels that contain strong carbide-forming elements such as Nb, Ti, V, Cr, and Mo, fine alloy carbides nucleate on migrating α /austenite (γ) boundaries repeatedly, leading to characteristic rows of carbides or carbides on sheets parallel to the α/γ interface. This is called interphase precipitation.^[1] For weight saving of automobiles, demands for increasing strength of steel parts are increasing. Nanosized carbide dispersion via interphase precipitation has been applied to increase strength effectively. Funakawa *et al.*^[2] have recently developed a high-strength, low-carbon steel with good elongation by using nanosized interphase precipitation of Ti and Mo carbides. It was also reported that vanadium addition to medium-carbon steels for forging parts can strengthen proeutectoid α and pearlite by interphase precipitation of vanadium carbide (VC).^[3]

Several mechanisms of interphase precipitation have been proposed so far.^[1,4,5] Initially, Davenport and Honeycombe^[4] supposed that carbon is rejected from proeutectoid α to γ , and the resultant enrichment in γ adjacent to α causes nucleation of carbide at the α/γ interface. However, this model cannot explain why carbides are precipitated on sheets parallel to the interface because nucleation of carbide on immobile interface is necessary to form carbides on sheets.

Later, Honeycombe^[1] proposed ledge mechanism (Figure 1(a)). He proposed that the α/γ interface consists of immobile coherent plane (terrace) and mobile incoherent plane (ledge or riser), and then carbides nucleate at immobile terrace planes. In this ledge mechanism, it was assumed that α holds Kurdjumov-Sachs (K-S) orientation relationship (OR) such as $((111)_\gamma // (011)_\alpha, [\bar{1}01]_\gamma // [\bar{1}\bar{1}1]_\alpha)$ and the coherent terrace plane corresponds to close-packed planes in parallel relation, $(111)_\gamma // (011)_\alpha$. This model can explain straight sheet planes because sheet planes of carbide are fixed to be $(011)_\alpha$.

On the other hand, it was frequently observed that sheets of interphase precipitation are curved as schematically shown in Figure 1(b). The ledge mechanism is unable to explain such a curved sheet plane; thus, a quasi-ledge mechanism was proposed by Ricks and Howell.^[5] They supposed that originally, the incoherent and mobile interface is immobilized by carbide pinning on the interface. Bulging of an interface between particles with relatively large interparticle spacing and subsequent nucleation of carbide on the bulged interface generates next sheet in this model. Accordingly, interphase precipitation can occur at a α/γ interface with irrational OR and irrational orientation plane in this mechanism.

Recently, Okamoto *et al.*^[6] found that the sheet plane of interphase precipitation of NbC in low-carbon steel

GORO MIYAMOTO and TADASHI FURUHARA, are with the Institute for Materials Research, Tohoku University, Sendai, Miyagi 980-8577, Japan, and with the Consortium of the Japan Research and Development Center for Metals for Fundamental Studies on Technologies for Steel Materials with Enhanced Strength and Functions, Tokyo, Japan. Contact e-mail: miyamoto@imr.tohoku.ac.jp RYOTA HORI, formerly Graduate Student, Tohoku University, is now with Toyota Motor Corporation, Toyota, Aichi 471-8571, Japan. BEHRANG POORGANJI is with Robert R. McCormick School of Engineering & Applied Science, Northwestern University, Evanston, IL 60208-3100, and with the Consortium of the Japan Research and Development Center for Metals for Fundamental Studies on Technologies for Steel Materials with Enhanced Strength and Functions. Manuscript submitted October 8, 2012.

Article published online March 22, 2013

does not coincide with the $\{011\}_\alpha$ plane. Yen *et al.*^[7] also reported that orientation of sheet plane of carbide in Ti-Mo-bearing low-carbon steel is not close to $\{011\}_\alpha$ but is close to $\{211\}_\alpha$, $\{210\}_\alpha$, or $\{111\}_\alpha$. Those results indicate that ledge mechanism proposed by Honeycombe^[1] cannot be applied to the interphase precipitation of low-carbon steels.

In contrast to the sheet orientation, OR between α and γ and its effect on interphase precipitation has not been clarified well yet, although OR is fundamental factor to understand nature of the α/γ interface. This is because volume fraction of γ retained at room temperature is not sufficient to measure its orientation in ordinary low-carbon, low-alloy steels. Ryder *et al.*^[8] investigated the OR between α and γ by using a Co-Fe alloy where untransformed γ matrix does not transform into martensite and reported that the grain boundary α (GB- α) nucleated at γ boundary tends to hold specific OR with at least one side of γ . Law *et al.*^[9] investigated OR between a small amount of retained γ and GB- α in V-added low-carbon steel by using selected-area diffraction analysis in transmission electron microscopy (TEM) observation. They concluded that interphase precipitation can occur at GB- α/γ interface irrespective ORs. However, determination of orientation based on selected-area diffraction is not so accurate when the amount of retained γ is quite low. Furthermore, it is usually difficult for TEM observation to clarify growth direction of GB- α because the observation area is small and limited.

The electron backscattering diffraction (EBSD) technique has been widely used nowadays to analyze phase transformation.^[10] Because martensite holds nearly K-S OR with γ , the OR relationship between α and γ can be investigated indirectly by comparing the orientations of martensite and α .^[11,12] Recently, the current authors developed a novel method to determine the orientation of prior γ grain accurately.^[13] This method is based on numerical fitting of pole figures of martensite and does

not need a presence of retained γ . It has been applied to OR analysis of reversely formed γ from pearlite structure^[14] or reconstruction of γ orientation map.^[15]

Therefore, in this article, we aim to investigate crystallography of the α/γ interface to discuss the mechanism of interphase precipitation in V-added medium-carbon steel.

II. EXPERIMENTAL PROCEDURE

Plain and V-added medium-carbon steels containing 0.3 mass pct V were used. Those alloys are referred as base and V-added alloys, respectively. Nominal compositions and A_{e3} , A_{e1} , and dissolution temperatures of V(C,N) for those alloys calculated by using ThermoCalc (Thermo-Calc, Stockholm, Sweden) are shown in Table I. Homogenization treatment of the alloys was performed at 1453 K (1180 °C) for 172.8 ks in silica tube encapsulated with Ar gas to avoid decarburization. Then, those specimens were austenitized for 0.6 ks at 1423 K (1150 °C) for the base alloy or at 1473 K (1200 °C) for the V-added alloy and subsequently transformed isothermally in a salt bath at 973 K (700 °C) for 1.8 ks, followed by quenching into water. Similar nominal grain sizes of prior γ , about 390 μm , were obtained by the above treatments in the two alloys.

The α orientation maps were measured by EBSD at an accelerating voltage of 25 kV by using a scanning electron microscope (SEM; FEI Quanta 3D; FEI Corporation, Portland, OR). The data obtained by EBSD were analyzed with software for automatic crystal orientation mapping (OIM Analysis by TSL; EDAX, Inc., Mahwah, NJ). The specimens for EBSD measurements were prepared by mechanical polishing followed by electropolishing by using a solution of 100 g CrO_3 + 20 mL H_2O + 500 mL CH_3COOH . TEM thin-foil specimens were obtained by microsampling technique with a focused ion beam (FIB) facility. These thin

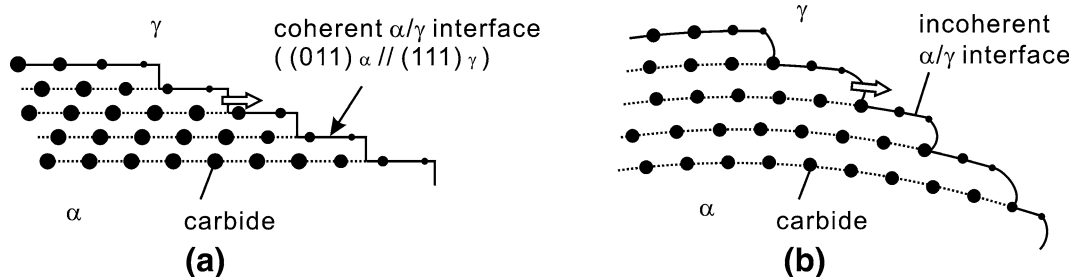


Fig. 1—Models for interphase precipitation of carbide. (a) Ledge mechanism for straight sheet of carbide.^[1] (b) Quasi-ledge mechanism for curved sheet of carbides^[5].

Table I. Chemical Compositions and A_{e3} , A_{e1} , and Dissolution Temperatures of V(C,N) for the Alloys Calculated by Using ThermoCalc

| | C | Si | Mn | V | P | S | Al | N | Fe | Para- A_{e3} (K) | Para- A_{e1} (K) | Dissolution Temperature of V(C,N) (K) |
|------------|------|------|------|--------|-------|-------|-------|--------|------|-----------------------|-----------------------|------------------------------------------|
| Base Alloy | 0.44 | 0.26 | 0.86 | <0.005 | 0.015 | 0.013 | 0.029 | 0.0041 | bal. | 1025 | 983 | — |
| V-Added | 0.44 | 0.25 | 0.85 | 0.29 | 0.014 | 0.016 | 0.030 | 0.0044 | bal. | 1035 | 986 | 1383 |

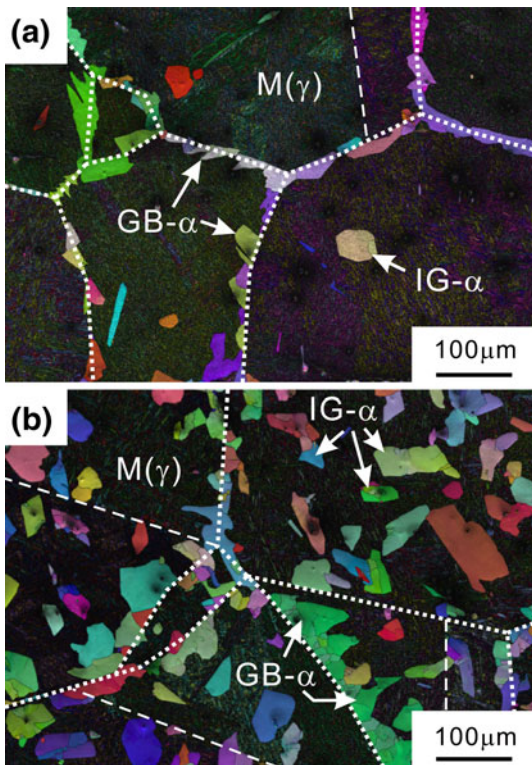


Fig. 2— α orientation maps superimposed with IQ map: (a) base alloy transformed at 973 K (700 °C) for 1.8 ks and (b) V-added alloy transformed at 973 K (700 °C) for 1.8 ks. Dashed and broken lines represent prior γ grain boundaries and annealing twin boundaries, respectively.

foils were observed with TEM (Philips CM300; Philips, Amsterdam, the Netherlands) operated at 300 kV.

III. RESULTS

A. OR Between γ and Proeutectoid α

Figure 2 shows α orientation map superimposed with image quality (IQ) maps. Bright-colored (high IQ) and dark (low IQ) regions correspond to proeutectoid α and untransformed γ , which is now transformed to martensite, respectively. In the base alloy, proeutectoid α are mostly nucleated at prior γ grain boundaries as shown in Figure 2(a). By the addition of 0.3 pct V, the formation of intragranular α (IG- α) is promoted, as previously reported.^[16,17] From these orientation data, the ORs between proeutectoid α and γ are analyzed.

Figure 3 shows examples of the analysis. Four GB- α , α_1 , and α_2 in the base alloy (Figure 3(a)) and α_3 and α_4 in the V-added alloy (Figure 3(e)) are selected. Orientations of martensite transformed from neighboring γ grains, γ_1 and γ_2 in the base alloy, and γ_3 and γ_4 in the V-added alloy, are shown as black points in $\{001\}_{\text{bcc}}$ (body-centered cubic [bcc]) pole figures of Figures 3(b), (c), (f) and (g), respectively. The $\{001\}$ poles obtained from GB- α are plotted on those figures as colored circles. Because martensite holds ORs close to the K-S OR with γ , $\{001\}_{\text{bcc}}$ pole figures of martensite exhibit a

characteristic pattern, which is called a K-S pattern hereafter. If a selected α holds near-K-S OR with γ , then orientation of the α coincides with the K-S pattern. Thus, whether the α holds close to K-S OR with γ or not can be easily identified by comparing α orientation and K-S pattern. As shown in Figure 3(b), orientations of α_1 and α_2 agree well with the K-S pattern of γ_1 , indicating that those GB- α hold close to K-S OR with γ_1 . Figure 3(c) shows that α_2 also holds near-K-S OR with γ_2 while orientation of α_1 does not coincide with the K-S pattern of γ_2 . To investigate deviation from the exact K-S OR more quantitatively, the orientation matrix of γ (M^{fcc} ; face-centered cubic [fcc]) is calculated from those of martensite according to a previous study.^[13] Then, a deviation angle ($\Delta\theta$) of α/γ from the exact K-S OR is estimated from the following equations:

$$\Delta\theta = M^{\text{K-S}}(C_n M^{\text{fcc}})(C_m M^{\text{bcc}})^{-1}$$

where C_n and C_m are conversion matrices of the basic axes and n and m vary from 1 to 24. M^{bcc} and $M^{\text{K-S}}$ are the orientation matrices of GB- α and OR matrix for the exact K-S OR, respectively. The table in Figure 3(d) shows the deviation angles of α_1 and α_2 from the exact K-S OR with respect to γ_1 and γ_2 . The deviation angles among α_1/γ_1 , α_2/γ_1 , and α_2/γ_2 are small, while that for α_1/γ_2 is large. In the present analysis, 5 deg is taken as a threshold between near-K-S/non-K-S OR; i.e., α with $\Delta\theta$ less than 5 deg is considered to hold near-K-S OR and vice versa. Figures 3(f) through (h) show α_3 and α_4 hold near-K-S OR with at least one of the adjacent γ grains.

The symbols of circles and triangles in Figures 3(a) and (e) show whether GB- α hold near-K-S OR with γ ($\Delta\theta < 5$ deg) or not ($\Delta\theta > 5$ deg), respectively, where blue and red colors indicate OR with upper γ (γ_1) and lower γ (γ_2). It is clearly seen that most of the α grains have near-K-S OR with at least one side of γ both in the base and V-added alloys. A large difference between two alloys is that some GB- α holds K-S OR with both sides of γ in the base alloy while there is no such GB- α in the V-added alloy. Furthermore, Figure 3(a) clearly shows that GB- α can grow into both near-K-S and non-K-S sides in the base alloy while interfaces holding near-K-S OR in the V-added alloy hardly migrate during α transformation and α grains grow into only non-K-S side as shown in Figure 3(e).

Figure 4 summarizes ORs between GB- α and γ . n in Figures 4(b) and (c) indicates the number of GB- α analyzed at 11 and 3 different grain boundaries for V-free and V-added alloys, respectively. As shown in Figure 4(a), misorientation angles from the K-S OR with either side of γ are represented by $\Delta\theta_1$ and $\Delta\theta_2$ where $\Delta\theta_1 < \Delta\theta_2$. $\Delta\theta_1$ and $\Delta\theta_2$ in the base and V-added alloys are shown in Figures 4(b) and (c), respectively. As summarized in Figure 4(d), the fractions of GB- α with $\Delta\theta_1 < 5$ deg, which correspond to α holding near-K-S OR with at least one adjacent γ grain, are about 75 pct, and the fraction is similar in the two alloys. In contrast, the fraction of the GB- α with $\Delta\theta_2 < 5$ deg in the V-added alloy, which indicates that GB- α holding near-K-S OR with both sides of γ , is much fewer than that in the base alloy. Figure 5 shows $\Delta\theta$ for the IG- α , which

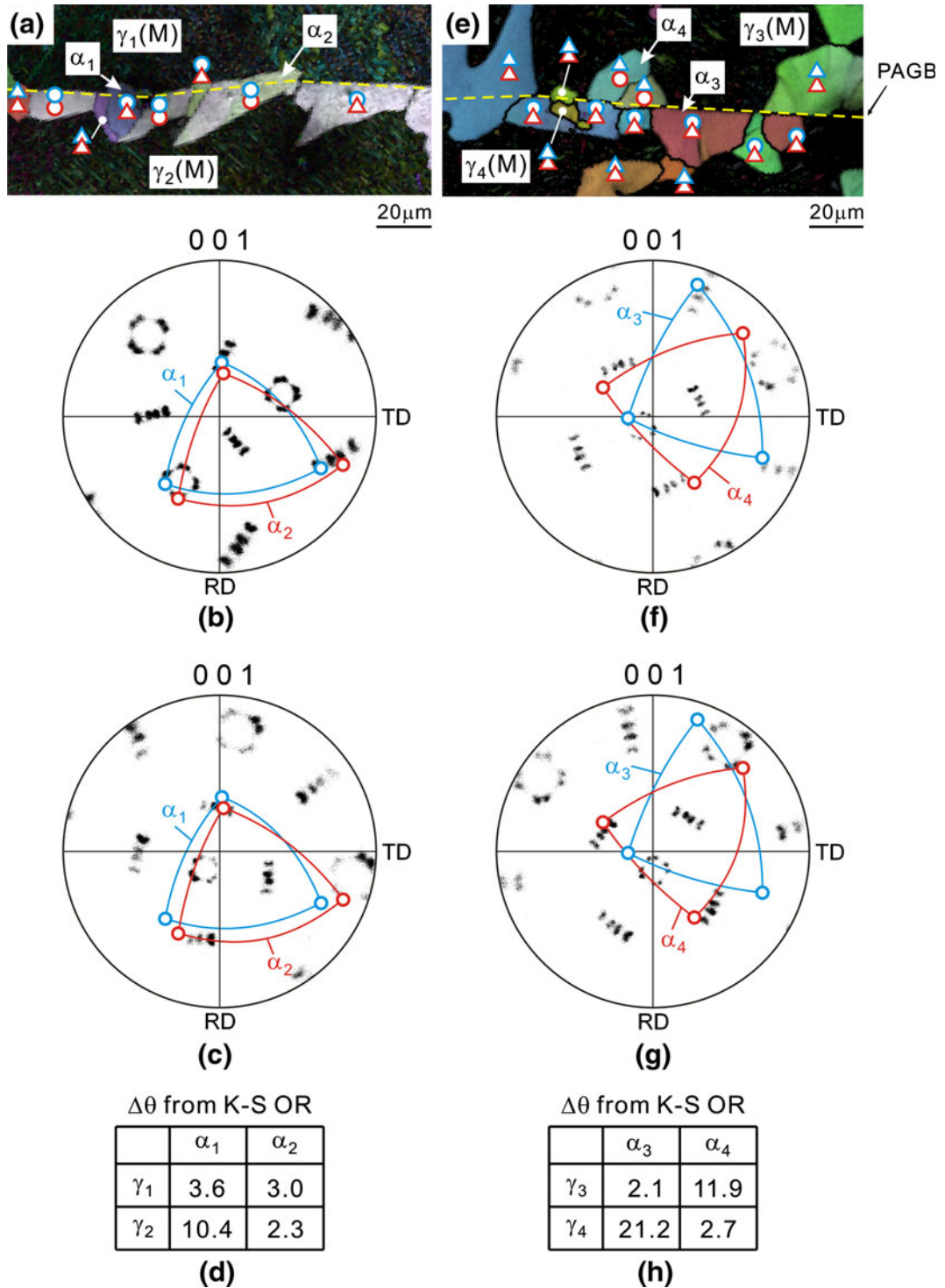


Fig. 3—Base alloy (a) α orientation + IQ map, (b) $\{001\}_\alpha$ pole figure of α_1 and α_2 , martensite in γ_1 , (c) $\{001\}_\alpha$ pole figure of α_1 and α_2 , martensite in γ_2 , and (d) table showing deviation angle from exact K-S OR between α and γ . (e) through (h) correspond to the V-added alloy (Color figure online).

are presumably nucleated at inclusions in both alloys. Regardless of the V addition, $\Delta\theta$ for all the IG- α grains are larger than 5 deg. Such a large deviation from the K-S OR is also consistent with the features reported previously.^[12,17]

Those results indicate that proeutectoid α transformation in the V-added alloy proceeds dominantly by the migration of non-K-S interface.

A plane orientation of the α/γ interface is also important to consider the character of the interface.

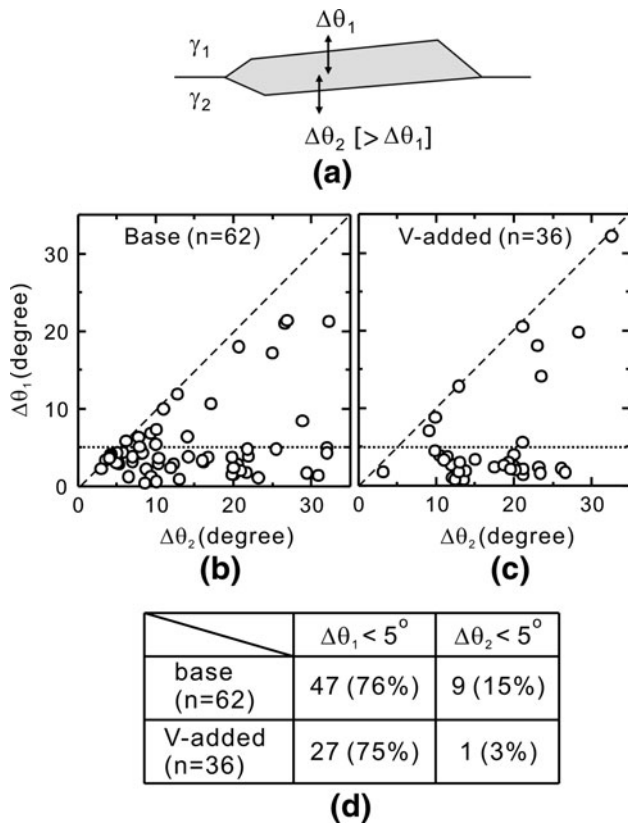


Fig. 4—(a) Schematic illustration of GB- α , $\Delta\theta$ plot of GB- α , (b) in the base alloy, (c) in the V-added alloy, and (d) the number of GB- α holding near-K-S OR with respect to adjacent γ grains.

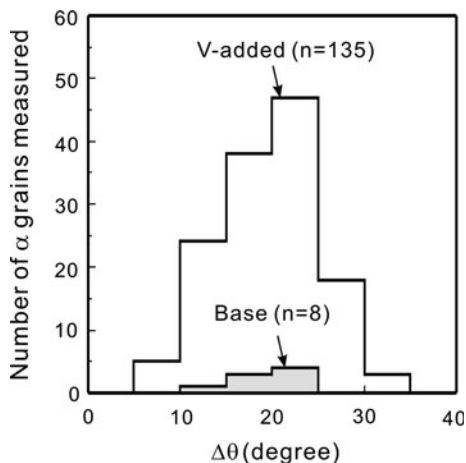


Fig. 5—Histogram of the number of α in the base and V-added alloys as a function of $\Delta\theta$.

To determine an interface orientation uniquely, a trace analysis in two different planes is necessary. Therefore, first, a trace of α/γ interface is observed in the etched surface after EBSD measurement (Figure 6(b)). Then, the plane perpendicular to the surface was made by using FIB as shown in Figure 6(c) to observe the trace of the interface on another plane. The orientation of interface can be determined from those two trace

directions (Figure 6(a)). By using α and γ orientations acquired from the EBSD measurement, the plane orientation of the interface was calculated in both α and γ coordinates.

Figures 7(a) through (d) show interface normal directions in γ (Figure 7(a), base alloy and Figure 7(c), V-added alloy) and α (Figure 7(b), base alloy and Figure 7(d), V-added alloy). The open and solid circles indicate near the K-S and non-K-S interfaces, respectively. According to the ledge mechanism, the interface orientations of α/γ interfaces should be nearly parallel to the close-packed planes in parallel relationship, $\{111\}_\gamma$ and $\{011\}_\alpha$. Actually, the macroscopic habit plane, as expected, deviates slightly by the introduction of regularly aligned atomistic steps with the terrace plane of $(111)_\gamma // (011)_\alpha$.^[18] However, interface orientations are randomly scattered and do not match the well-characterized habit plane mentioned above in terms of both α and γ orientations regardless of OR.

IV. DISCUSSION

A. Effects of V Addition on OR Between α and γ

The current authors previously reported that the OR between GB- α and γ in a low-carbon steel are more randomized by the V addition and pointed out that α nucleation on VC can lead to the randomization of OR between GB- α and γ .^[19,20] Similarly, in the present study, the fraction of GB- α holding near-K-S OR with both sides of γ grains is decreased by the V-addition although GB- α in the V-added alloy tends to hold near-K-S OR with at least one side of γ similarly to the base alloy (Figure 4(d)). Furthermore, a significant effect of V addition appears in the growth direction of α in this study; a part of the K-S interface can migrate in the base alloy, while GB- α in the V-added alloy does not grow into the near-K-S side. Therefore, in addition to the randomization by α nucleation on VC, such retarding effect of V on the migration of the K-S interface can be a reason why a α grain holding near-K-S OR with both sides of γ grains was not observed in the V-added alloy.

Either solute drag by segregation of V or pinning by VC particles may reduce a mobility of the near-K-S interface. Because coherent grain boundary has a lesser interaction with solute atoms than random boundaries in general,^[21] solute drag of V cannot explain strong retardation only for the coherent K-S interface. Accordingly, precipitation of VC at the interface and resultant pinning effect should play an important role in restricting growth direction, although details are not clear at present.

B. Mechanism of Interphase Precipitation of VC

Migrating α/γ interfaces act as a nucleation site for interphase precipitation. In this study, it was found that the α/γ interfaces without K-S OR migrate dominantly during growth of the GB- α and IG- α in the V-added alloy. Furthermore, the plane orientations of α/γ interfaces are not parallel to the specific crystallographic

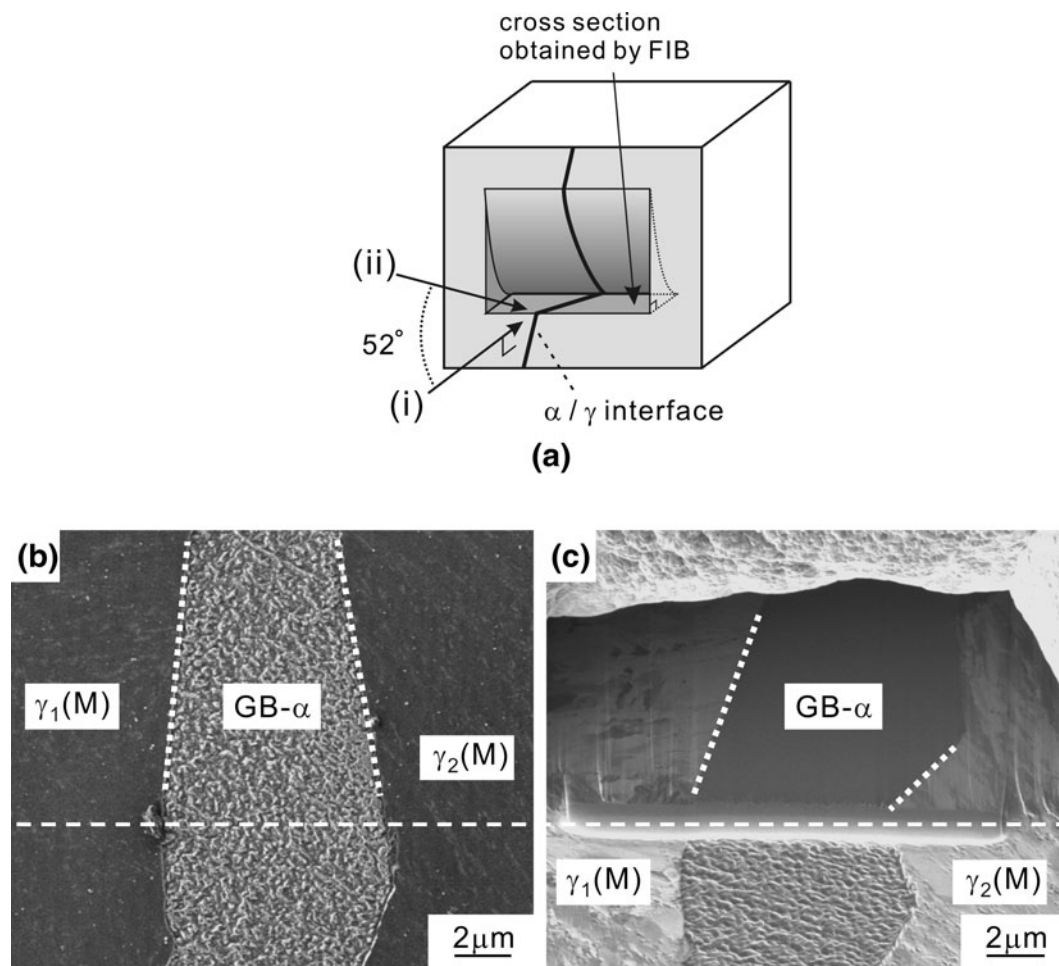


Fig. 6—(a) Schematic illustration of trace analysis on two planes for determining normal direction of α/γ interface by using FIB. (b) Scanning ion microscopy (SIM) image observed along the direction (i). (c) SIM image observed along the direction of (ii) after FIB patterning.

planes both in terms of α and γ orientation. Those results indicate that ledge mechanism for interphase precipitation originally proposed by Honeycombe^[1] cannot be applied to the V-added medium-carbon steel investigated in this study.

Figure 8 shows TEM images of interphase precipitation of VC particles in IG- α in the V-added alloy. Two thin-foil specimens are taken from regions A and B by using FIB from an identical IG- α shown in Figure 8(a). $\Delta\theta$ of this IG- α is 21.7 deg, so that OR is far apart from the K-S OR. As shown in dark-field images of Figures 8(b) and (c), interphase precipitation of VC is observed. Although sheet planes are not well recognized due to coarsening of VC particles, carbide sheets are parallel to the α/γ interface in both regions. VC particles have Baker-Nutting (B-N) OR $((001)_\alpha // (001)_{VC}, [110]_\alpha // [100]_{VC})$ with respect to α grain, and only one variant among three possible variants of the B-N OR is formed in both regions of A and B, while the observed variant is different from each other. It was clarified that the habit plane of the observed variants are closer to the α/γ interface than these for the other two variants. Different sheet orientation is found even in the same α grain; thus,

the same OR between α and γ does not agree with the ledge mechanism.

It should be pointed out also that straight sheets of VC are observed in the same specimen,^[3] the formation of which cannot be explained by the quasi-ledge mechanism. Furuhashi and Maki^[22] investigated the interfacial structure of fcc matrix and bcc precipitate at fcc grain boundaries and found that the non-K-S interface is composed of ledge structure. This implies that the α/γ interface without holding the K-S OR also contains partially coherent planes with low mobility. Indeed, Furuhashi *et al.*^[23] reported that a grain boundary bcc precipitate tends to form major facets with higher geometrical atomic matchings in both near-K-S ORs and non-K-S ORs. It is considered that such facet orientations correspond to local minima of interface mobility. Therefore, the ledge mechanism proposed by Honeycombe can be extended to the non-K-S interface.

When atomic matching of a given α/γ interface orientation is much better than those of other nearby oriented planes, a mobility of this plane is much less than the others. This leads to well developed facet as indicated by type A in Figure 9(a). If several closely

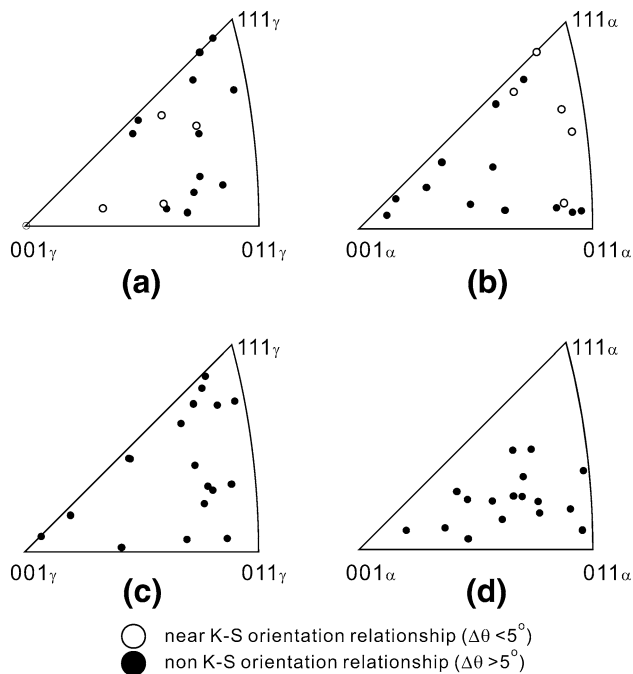


Fig. 7—Standard stereographic projection showing normal directions of migrating α/γ interfaces: (a) the base alloy in γ direction and (b) in α direction, (c) the V-added alloy in γ direction and (d) in α direction.

oriented α/γ interfaces have similar atomic matching and thus mobility, then the macroscopic α/γ interface consists of several plane orientations, resulting in the formation of curved interface (type B in Figure 9(c)). Furuhashi *et al.*^[23] reported on a basis of a nearest coincide site model analysis that there can be several interface directions with good atomic matching for a given irrational OR between α/γ . Their calculations support that interface structure between given α and γ grains can be varied place to place, although it has not been verified experimentally.

Because the height of ledge is usually less than or about 1 nm, interphase precipitation does not take place on every ledge but does occur once every ten ledges to form carbides on sheets with intersheet spacing of about 10 to 20 nm in this specimen.^[3] The present authors have recently proposed that dynamical segregation of V atoms on migrating α/γ interface is a trigger for nucleation of VC.^[24]

- Migration of α/γ interface occurs dominantly in a ledge-wise growth mode of which terrace plane is less mobile than riser. But a part of terrace plane is bowed out gradually between particles with relatively large interparticle spacing. V content at the interface increases due to segregation of V and thus growth rate decreases by the solute drag effect.
- When V content at the interface reaches the critical value, VC particles are nucleated on this interface, causing the interface to be pinned.
- Subsequently, other carbides are nucleated on the pinned interface until segregated V atoms disappear.

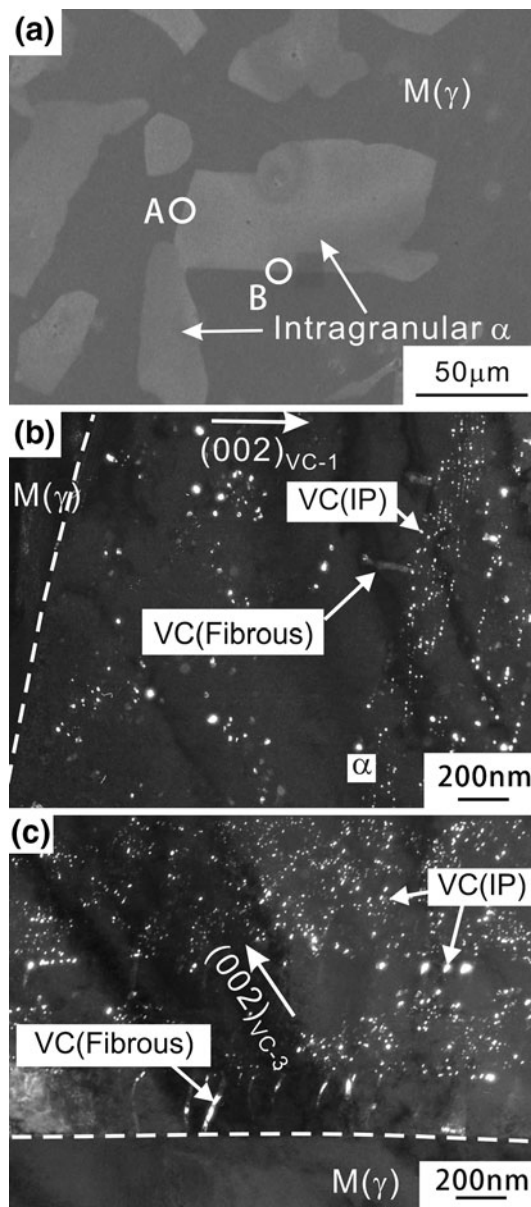


Fig. 8—(a) SIM image of IG- α in the V-added alloy; (b) dark-field TEM image of VC at the region A, which is taken from $(002)_{VC-1}$ reflection; (c) dark-field TEM image of VC at the region B, which is taken from $(002)_{VC-3}$ reflection.

Reactions (a) through (c) were repeated to generate carbides in rows parallel to the α/γ interface. This model is based on ledge mechanism, but it can be also considered as bowing mechanism by taking the difference of interfacial mobility into account. According to this mechanism, the kinetics of segregation of V and nucleation of VC determine intersheet spacing so that the intersheet spacing varies α grain to grain or even within the α grains due to gradual change in the growth rate of α in addition to the difference in interface character.

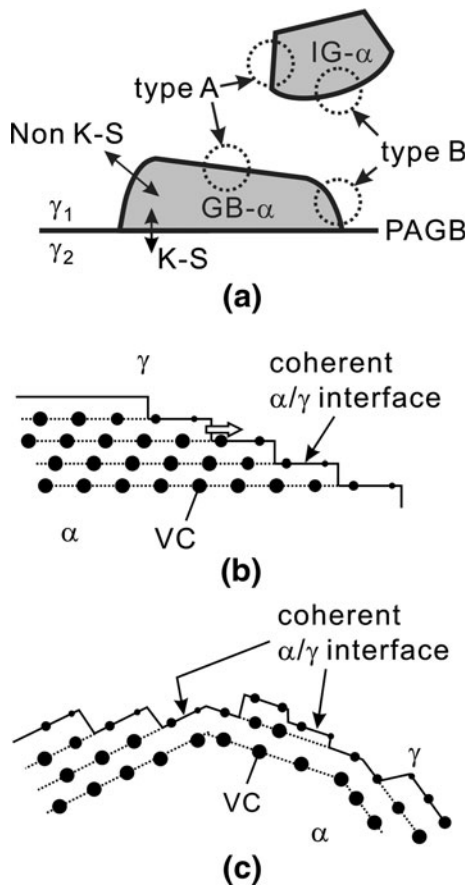


Fig. 9—(a) Schematic illustration of GB- α and IG- α in the V-added alloy, (b) type A interface with straight sheet, and (c) type B interface with curved sheet.

V. CONCLUSIONS

The α/γ ORs and orientations of α/γ interface were investigated in the V-free and V-added medium-carbon steels transformed at 973 K (700 °C). The obtained results are summarized as follows:

1. A large part of grain boundary α holds near-K-S OR with at least one side of austenite adjacent to grain boundary regardless of V addition. By the V addition, a fraction of grain boundary α holding near-K-S OR with both sides of γ is decreased remarkably. Furthermore, only non-K-S α/γ interfaces migrate dominantly in the V-added alloy in contrast to the V-free alloy.
2. All the intragranular α , presumably formed at the inclusion, does not hold K-S OR with γ both in V-free and V-added alloys.
3. α/γ interface orientations are not fixed crystallographically but are randomly distributed in terms of α and γ orientation.
4. The above results do not agree with the ledge mechanism originally proposed by Honeycombe. It is proposed that the ledge mechanism can be extended

to the non-K-S interface that partially consists of coherent and less-mobile interface.

ACKNOWLEDGMENT

This study was conducted as a part of the R&D on Fundamental Technology for Steel Materials with Enhanced Strength and Functionality funded by the New Energy and Industrial Technology Development Organization (NEDO).

REFERENCES

1. R.W.K. Honeycombe: *Phase Transformation in Ferrous Alloy*, A.R. Marder and J.I. Goldstein, eds., TMS, Warrendale, PA, 1984, p. 49.
2. Y. Funakawa, T. Shiozaki, K. Tomita, T. Yamamoto, and E. Maeda: *ISIJ Int.*, 2004, vol. 44, pp. 1945–51.
3. G. Miyamoto, R. Hori, B. Poorganji, and T. Furuhashi: *ISIJ Int.*, 2011, vol. 51, pp. 1733–39.
4. A.T. Davenport and R.W.K. Honeycombe: *Proc. R. Soc. Lond. A*, 1971, vol. 322, pp. 191–205.
5. R.A. Ricks and P.R. Howell: *Acta Metall.*, 1983, vol. 31, pp. 853–61.
6. R. Okamoto, A. Borgenstam, and J. Agren: *Acta Mater.*, 2010, vol. 58, pp. 4783–90.
7. H.W. Yen, P.-Y. Chen, C.Y. Huang, and J.R. Yang: *Acta Mater.*, 2011, vol. 59, pp. 6264–74.
8. P.L. Ryder, W. Pitsch, and R.F. Mehl: *Acta Metall.*, 1967, vol. 15, p. 2.
9. N.C. Law, S.A. Parsons, P.R. Howell, and D.V. Edmonds: *Mater. Sci. Technol.*, 1987, vol. 3, pp. 642–48.
10. A. Lambert-Perlade, A.F. Gourgues, and A. Pineau: *Int. Mater. Rev.*, 2007, vol. 52, pp. 65–128.
11. T. Furuhashi, T. Shinyoshi, G. Miyamoto, J. Yamaguchi, N. Sugita, N. Kimura, N. Takemura, and T. Maki: *ISIJ Int.*, 2003, vol. 43, pp. 2028–37.
12. G. Miyamoto, T. Shinyoshi, J. Yamaguchi, T. Furuhashi, T. Maki, and R. Uemori: *Scripta Mater.*, 2003, vol. 48, pp. 371–77.
13. G. Miyamoto, N. Takayama, and T. Furuhashi: *Scripta Mater.*, 2009, vol. 60, pp. 1113–16.
14. Z.D. Li, G. Miyamoto, Z.G. Yang, and T. Furuhashi: *Scripta Mater.*, 2009, vol. 60, pp. 485–48.
15. G. Miyamoto, N. Iwata, N. Takayama, and T. Furuhashi: *Acta Mater.*, 2010, vol. 58, pp. 6393–403.
16. F. Ishikawa, T. Takahashi, and T. Ochi: *Metall. Mater. Trans. A*, 1994, vol. 25A, pp. 929–36.
17. T. Furuhashi, J. Yamaguchi, N. Sugita, G. Miyamoto, and T. Maki: *ISIJ Int.*, 2003, vol. 43, pp. 1630–39.
18. T. Furuhashi, K. Wada, and T. Maki: *Metall. Mater. Trans. A*, 1995, vol. 26A, pp. 971–78.
19. T. Furuhashi, G. Miyamoto, H. Saito, and T. Maki: *Solid-Solid Phase Transformation in Inorganic Materials (PTM2005)*, 2005, p. 5.
20. T. Furuhashi, H. Saito, G. Miyamoto, and T. Maki: *Mater. Sci. Forum*, 2010, vols. 654–656, pp. 1–6.
21. L.E. Murr: *Interfacial Phenomena in Metals and Alloys*, Addison-Wesley, Reading, MA, 1975, p. 328.
22. T. Furuhashi and T. Maki: *Mater. Trans. JIM*, 1992, vol. 33, p. 734.
23. T. Furuhashi, K. Oishi, and T. Maki: *Metall. Mater. Trans. A*, 2002, vol. 33A, pp. 2327–35.
24. T. Murakami, H. Hatano, G. Miyamoto, and T. Furuhashi: *ISIJ Int.*, 2012, vol. 52, pp. 616–25.